Research Article Vol. 36, No. 2 / February 2019 / Journal of the Optical Society of America B 243

Journal of the Optical Society of America B

OPTICAL PHYSICS

Frequency stabilization of a 650 nm laser to an I_2 spectrum for trapped $^{138}Ba^+$ ions

Tian Xie,[1,2] Naijun Jin,[1,2] Ye Wang,[1] Junhua Zhang,[3,1] Mark Um,[1] Pengfei Wang,[1] and Kihwan Kim[1,*]

[1]Center for Quantum Information, Institute for Interdisciplinary Information Sciences, Tsinghua University, Beijing 100084, China
[2]Department of Physics, Tsinghua University, Beijing 100084, China
[3]Shenzhen Institute for Quantum Science and Engineering, and Department of Physics, Southern University of Science and Technology, Shenzhen, China
*Corresponding author: kimkihwan@mail.tsinghua.edu.cn

Received 18 May 2018; revised 25 November 2018; accepted 3 December 2018; posted 4 December 2018 (Doc. ID 331944); published 15 January 2019

Optical manipulation of Ba^+ ions is performed mainly by a 493 nm laser for the $S_{1/2}$ – $P_{1/2}$ transition and a 650 nm laser for the $P_{1/2}$ – $D_{3/2}$ transition. Because the branching ratio between the 493 and 650 nm transitions of a single Ba^+ ion is comparable, stabilization systems of both lasers are equally important for Doppler cooling, sub-Doppler cooling, optical pumping, and state detection. The stabilization system of a 493 nm laser to an absolute Te_2 reference has been well established. However, the stabilization of a 650 nm laser to the absolute reference of an atomic or molecular spectrum has not been presented before, to our knowledge. Here, we experimentally obtain the I_2 spectrum near 650 nm and provide the experimental connection to the spectrum of Ba^+. We present the 20 spectral lines of I_2 in the range of 0.9 GHz above the resonance of the $P_{1/2}$ – $D_{3/2}$ transition. We stabilize the 650 nm laser through the optical cavity to the lowest one among these lines, which is about 350 MHz apart, as the absolute frequency reference. Finally, we measure the frequency differences between these iodine lines and the Ba^+ resonance through the fluorescence excitation spectrum with well-resolved dark states, which is in agreement with the theoretical expectation. The presented stabilization scheme enables us to perform precise experiments with Ba^+ ions.

https://doi.org/10.1364/JOSAB.36.000243

1. INTRODUCTION

Recently, ion-trap systems have been greatly developed for quantum computation [1–3], quantum simulation [4,5], and fundamental tests of quantum mechanics [6–8], where accurate and precise control is required. Because the states of ions are mainly manipulated by optical methods, it is essential to stabilize lasers, particularly in the frequency domain. The performance of a laser system is characterized by its linewidth and long-term drift of the frequency. To narrow the laser linewidth, a high-finesse cavity is typically used, for example in the Pound–Drever–Hall (PDH) method [9], but the long-term drift cannot be overcome in this way.

As a solution, atomic or molecular cells are usually used as the absolute reference for laser stabilization. In particular, hyperfine-resolved optical transitions of iodine (I_2) have been thoroughly studied [10,11], providing absolute references from the dissociation limit at 499.5 nm to the near-infrared region including the stabilization of 532, 605, 612, 633, 740, and 830 nm lasers [12–17]. Doppler-free spectroscopy, such as the saturated absorption spectroscopy (SAS) [18] or modulation transfer spectroscopy (MTS) [19], is widely used in laser stabilization systems, where the width of the error signal in the servoloop can be compressed to the tens of MHz level.

In the field of quantum computation [20,21], quantum communication [22], and precision measurement of parity nonconservation [23] with trapped ions, the Ba^+ ion has been an attractive choice. A single Ba^+ ion has low-lying and long-lived D states [24] and a lambda structure of cooling cycle [25], which are all in the visible wavelength range. A 493 nm laser drives the $S_{1/2}$ – $P_{1/2}$ transition, which performs as the main circulation of Doppler cooling. Because the branching ratios of the $P_{1/2}$ – $S_{1/2}$ and $P_{1/2}$ – $D_{3/2}$ transitions are comparable, 0.73 and 0.27 [26], respectively, a 650 nm laser bridging the $D_{3/2}$ – $P_{1/2}$ transition is in need to pump the population in $D_{3/2}$ state back to the cooling cycle. Stabilization of the 493 nm laser with tellurium (Te_2) as the absolute reference has been well-developed [27]. However, the 650 nm laser has been used without absolute stabilization, because a modest Doppler-cooling efficiency can be achieved by using a far red-detuned repumping laser. Looking forward, as we try to achieve the optimal cooling efficiency and improve the efficiency of optical pumping and quantum-state detection [28], which are both sensitive to the choice of the detuning of the

650 nm laser, the stability of the 650 nm laser must be reprioritized. Furthermore, sub-Doppler cooling by EIT or Sisyphus mechanism would critically require the stability of the 650 nm laser at an exact frequency [29,30]. The stabilization system of the 650 nm laser, however, has not been completely discussed [28,31].

In this work, we report 20 spectral lines of I_2 close to the $P_{1/2} - D_{3/2}$ transition of the $^{138}Ba^+$ ion at 649.87 nm from the MTS. By employing one of these lines as an absolute reference, we accomplish the absolute stabilization system of the 650 nm laser with the linewidth of ∼400 kHz. We also measure the spectrum of a single $^{138}Ba^+$ ion by scanning the frequency of the 650 nm laser with a fiber-coupled EOM while fixing the frequency of the 493 nm laser and comparing the results with the numerical simulation of the Liouville equation [32]. We conclude that the frequency of the reference line is 350 MHz higher than the resonance of the $P_{1/2} - D_{3/2}$ transition of the $^{138}Ba^+$ ion.

2. I_2 SPECTROSCOPY

In this section, we introduce the absolute stabilization system of the 650 nm laser and the MTS of I_2 as shown in Figs. 1 and 2. The whole system can be divided into two parts. We first narrow the linewidth of a Toptica DL100 prodiode laser by an optical cavity. We then stabilize the optical cavity to the absolute reference of I_2 by means of MTS to suppress its length drift, which is mainly caused by temperature fluctuation. The 18.4 mW output of the laser is split into four beams by one beam splitter (BS) and two polarizing beam splitters (PBS). 0.3 mW is used for a wavemeter from HighFinesse, 0.9 mW for the ion trap experiment, 3.5 mW for the optical cavity setup and the remaining 10 mW is coupled into a fiber-coupled EOM for the implementation of the MTS setup.

Due to the low efficiency of the fiber-coupled EOM, only 2 mW is available for the optical part of the MTS setup. The beam is adjustably split in two using a half wave plate (HWP) and a PBS. The transmitted beam from the PBS, the pump beam, is sent through an AOM and its +1st order output (430 μW) is selected. The reflection beam from the PBS (250 μW) goes through a convex lens and is then split into a reference beam (70 μW) and a probe beam (160 μW). The reference beam goes into one port of the balanced photodiode (balanced PD). The probe beam and the modulated pump beam counter propagate through an I_2 cell, which diminishes the effect of Doppler broadening by narrowing the velocity region of I_2 that can simultaneously interact with both beams. After that, the probe beam goes into the other port of the balanced PD. The PD output is sent to a lock-in amplifier.

To implement the phase-sensitive detection of our dispersive signal, we incorporate an AOM driven by a frequency-modulated signal from a voltage-controlled oscillator (VCO) which scans from 190–210 MHz at a scanning frequency of 10 kHz. This 10 kHz modulation signal also acts as the reference for the lock-in amplifier. We use a servo PID board to process the generated signal and stabilize the cavity length by controlling the piezo voltage. After locking, the linewidth of the laser frequency is ∼400 kHz, which is obtained by recording the PDH signal after locking and converting its standard deviation to frequency. We do not observe a long-term drift during the lock within the uncertainty of our wavemeter.

Figure 2 shows the dispersive signal generated by scanning the frequency of the repumping laser through a range of 1.2 GHz near 649.868 nm. This signal serves as a proper zero-crossing dispersive error signal for the servo system. The frequency shifting due to the offset frequency of the modulation signal provided by the VCO has been subtracted, and the absolute frequency has been calibrated with the Ba^+ ion spectroscopy that will be discussed later. We choose the first line as the absolute reference to perform the frequency stabilization for convenience.

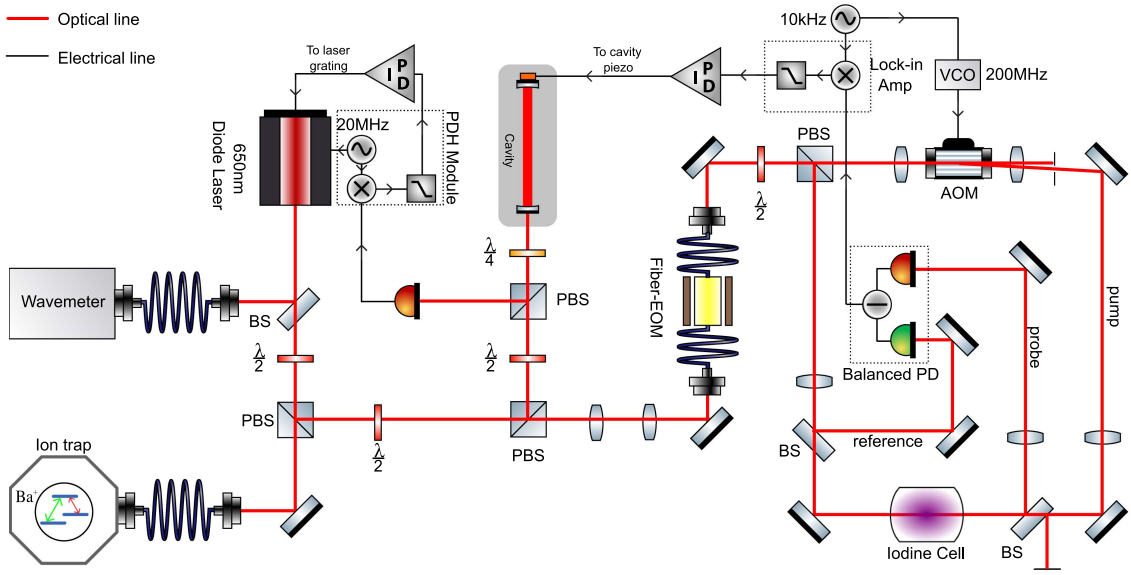

Fig. 1. Frequency stabilization system of the 650 nm laser to I_2 reference through an optical cavity. The thick red lines show the optical path and the thin black lines with arrows indicate electrical connections. The 493 nm laser system is omitted.

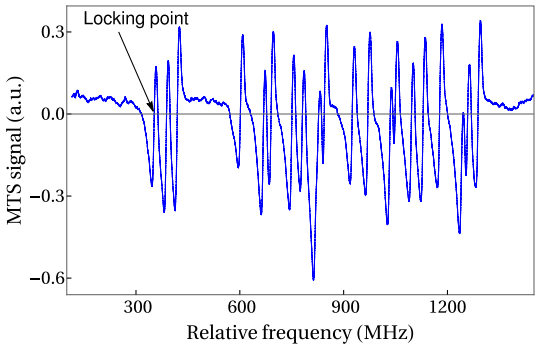

Fig. 2. Modulation transfer spectroscopy (MTS) signal of I_2 near the $P_{1/2} - D_{3/2}$ transition of $^{138}Ba^+$. Here the frequency axis shows the detuning between the absorption lines of I_2 and the resonance of $^{138}Ba^+$, which is determined by later experiments. The arrow indicates the locking point of the 650 nm laser.

3. $^{138}Ba^+$ SPECTROSCOPY

To determine the frequency differences between 20 lines and the resonance of the $P_{1/2} - D_{3/2}$ transition of the $^{138}Ba^+$ ion, we simulate the fluorescence excitation spectrum and compare it with the experimental results. We consider the situation that the detuning of the 493 nm laser is fixed and the detuning of the 650 nm is scanned. Figure 3 shows the lowest three energy levels of a single $^{138}Ba^+$ ion with its Zeeman sublevels. As mentioned in the introduction, the $S_{1/2} - P_{1/2}$ transition is the main cooling circulation. However, after a single ion is excited to the $P_{1/2}$ state, it has a non-negligible probability of decaying to the long-lived $D_{3/2}$ state, terminating the cooling cycle. Therefore, a 650 nm laser is necessary to repump the ion to the $P_{1/2}$ state. The repumping efficiency, which is related to the frequency of the 650 nm laser, greatly influences the cooling efficiency. To determine the repumping frequency, a single $^{138}Ba^+$ ion is loaded and excited from the $S_{1/2}$ ground state to the $P_{1/2}$ state by a 493 nm laser locked to a Te_2 reference. While scanning the frequency of the 650 nm laser, we measure the intensity of 493 nm fluorescence which can be interpreted as the repumping efficiency of the 650 nm laser as discussed above. In the following sections, we show the theory of fluorescence excitation spectrum and compare our experimental results with the numerical simulation.

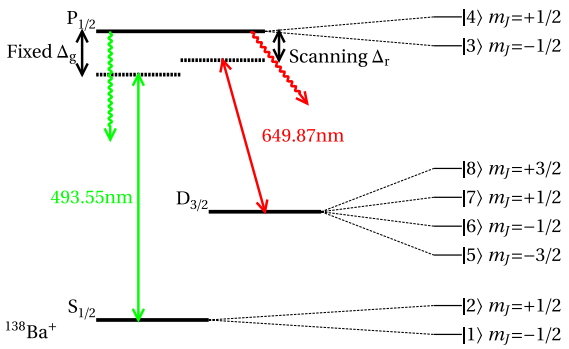

Fig. 3. Energy levels of the $^{138}Ba^+$ ion. In the presence of the magnetic field, the three-level system splits into an eight-level system. Δ_g (Δ_r) is the 493 (650) nm laser detuning from the resonance of the $^{138}Ba^+$ ion transition in the absence of Zeeman splitting. We label each state as $|i\rangle$ for the convenience of calculation.

A. Theory of the Fluorescence Excitation Spectrum

In the presence of a 5.8 Gauss magnetic field, the system can be described as an eight-level system [32]. By denoting each state shown in Fig. 3 as $|1\rangle, |2\rangle, \ldots, |8\rangle$, the atomic Hamiltonian can be expressed as

$$\hat{\mathcal{H}}_{\text{atom}} = \sum_{i=1}^{8} \hbar\omega_i |i\rangle\langle i|. \tag{1}$$

As for the interaction term, we treat two lasers as classical electromagnetic waves $\vec{E}_g \sin(\omega_g t)$ and $\vec{E}_r \sin(\omega_r t)$ because of their high intensity and assume that the light field only interacts with the electric dipole moment of the ion. By applying the rotating-wave approximation, the interaction Hamiltonian takes the form

$$\begin{aligned}\hat{\mathcal{H}}_{\text{int}} = -\frac{i}{2}[&\vec{E}_g \cdot (\vec{D}_{13}^{*}|3\rangle\langle 1| + \vec{D}_{14}^{*}|4\rangle\langle 1| + \ldots)e^{-i\omega_g t} \\ &+ \vec{E}_r \cdot (\vec{D}_{35}|3\rangle\langle 5| + \vec{D}_{36}|3\rangle\langle 6| + \ldots)e^{-i\omega_r t}] + \text{h.c.}.\end{aligned} \tag{2}$$

Here, $\vec{D}_{ij}$ is the electric dipole moment between state $|i\rangle$ and state $|j\rangle$. ω_r and ω_g are the frequencies of 493 and 650 nm laser beams, respectively. However, spontaneous decay exists in the system due to the interaction of the ion with the vacuum modes of the light field. A density matrix method should be employed to describe the whole system. The dynamic of this system is governed by the Liouville equation with a decay term [33]

$$\begin{aligned}\frac{d\hat{\rho}}{dt} &= -\frac{i}{\hbar}[\hat{\mathcal{H}}, \hat{\rho}] + \mathcal{L}_{\text{damp}}(\hat{\rho}) \\ \mathcal{L}_{\text{damp}}(\hat{\rho}) &= -\frac{1}{2}\sum_m [\hat{C}_m^{\dagger}\hat{C}_m\hat{\rho} + \hat{\rho}\hat{C}_m^{\dagger}\hat{C}_m - 2\hat{C}_m\hat{\rho}\hat{C}_m^{\dagger}].\end{aligned} \tag{3}$$

The general form of $\hat{C}_m = \sqrt{\Gamma_{ij}}|j\rangle\langle i|$ could summarize several different dissipative processes from $|i\rangle$ to $|j\rangle$ where Γ_{ij} is the decay parameter, including spontaneous decay from $P_{1/2}$ to $S_{1/2}$ or $D_{3/2}$ and the decoherence due to the finite linewidth of the driving light fields. In the experiment, we record the fluorescence photon number every 1 ms, in which case the system has already evolved into a steady state, and thus, all the elements in the density matrix could be numerically solved under the constraint conditions

$$\begin{aligned}\frac{d\hat{\rho}}{dt} = 0 \Rightarrow \frac{i}{\hbar}[\hat{\mathcal{H}}, \hat{\rho}] &= \mathcal{L}_{\text{damp}}(\hat{\rho}), \\ \text{tr}(\hat{\rho}) &= 1.\end{aligned} \tag{4}$$

The total fluorescence is proportional to $\rho_{33} + \rho_{44}$, the population of $P_{1/2}$ level. When the detuning difference between two lasers satisfies the condition for a Raman transition between specific Zeeman states of $S_{1/2}$ and $D_{3/2}$ [see Eq. (5)], the $P_{1/2}$ state will not be populated and no fluorescence will be detected. This effect, called dark resonance, results in a deep hole in the spectrum of the ion when scanning the frequency of one laser and fixing the other. When this condition is satisfied, the system will stay in a superposition state between the specific Zeeman sublevels of $S_{1/2}$ and $D_{3/2}$ levels, called a dark

state, which can be seen by calculating the off-diagonal terms of density matrix.

B. Measurement and Results

In the experiments, we keep the same linear polarization for both laser beams and use α to denote the angle between the polarization and the direction of the magnetic field. In the first case shown in Fig. 4, α is 45° with the 493 nm laser power of 1.5 μW and 650 nm laser power of 1.2 μW. We scan the frequency of the 650 nm laser while fixing the frequency of the 493 nm laser and obtain a spectrum close to the Lorentzian shape, as shown in Fig. 5. We find the frequency difference between the resonance of the $P_{1/2} - D_{3/2}$ transition and the locking point by fitting Fig. 5 with the simulated curve. For further tests, we adjust the laser polarization to be perpendicular to the magnetic field shown as the second case in Fig. 4, and obtain spectrums which contain characteristic dark states. Because there are only σ_+ and σ_- interactions in the second case, the dark state will occur when the detuning of the 650 nm laser satisfies

$$\Delta_r = \Delta_g \pm 3/5\frac{\mu_B|\vec{B}|}{\hbar}, \qquad \Delta_g \pm 11/5\frac{\mu_B|\vec{B}|}{\hbar}. \tag{5}$$

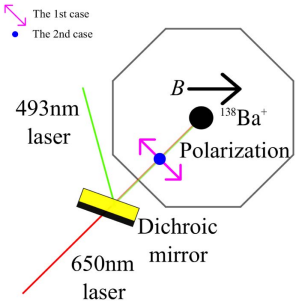

Fig. 4. Directions of the lasers and the magnetic field. In the first case, the polarizations of both lasers form 45° with the magnetic field. In the second case, the polarizations are perpendicular to the magnetic field.

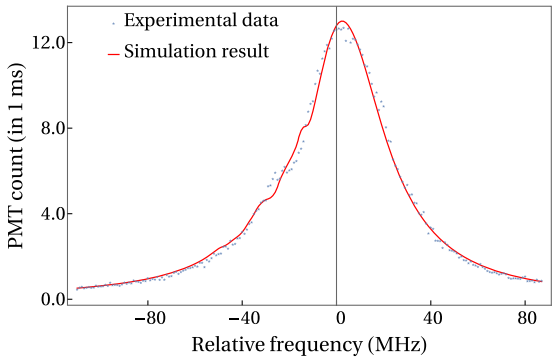

Fig. 5. Fluorescence excitation spectrum of a single $^{138}Ba^+$ ion by scanning the frequency of the 650 nm laser. Parameters are $\Delta_g/2\pi = -30$ MHz, $B = 5.8$G, 493 nm power = 1.5 μW, 650 nm power = 1.2 μW, $\alpha = 45°$, 493 linewidth = 0.3 MHz, 650 linewidth = 0.4 MHz.

In this case, the power of 493 and 650 nm lasers are 3.7 and 12 μW, respectively, and the result compared with the simulation shows in Fig. 6(a). And Fig. 6(b) shows the coherence terms, the off-diagonal elements in the density matrix between some specific sublevels of $S_{1/2}$ and $D_{3/2}$. In the experiment,

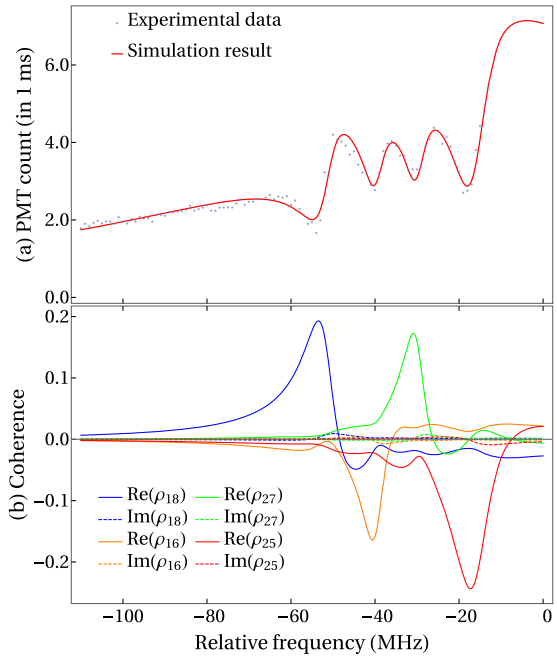

Fig. 6. Fluorescence excitation spectrum of a single $^{138}Ba^+$ ion, obtained by scanning the frequency of the 650 nm laser. Parameters are $\Delta_g/2\pi = -35$ MHz, $B = 5.8$G, 493 nm power = 3.7 μW, 650 nm power = 12 μW, $\alpha = 90°$, 493 linewidth = 0.3 MHz, 650 linewidth = 0.4 MHz. When the system is in a dark state, the ion will stay in a superposition state between specific Zeeman sublevels of the $S_{1/2}$ and $D_{3/2}$ state, which is obtained by calculating the off-diagonal terms of density matrix.

Table 1. Center Frequency of Each I_2 Line Relative to the Resonance of the $P_{1/2} - D_{3/2}$ Transition[a]

Num	Relative Freq (MHz)	Num	Relative Freq (MHz)
1	350	11	925
2	386	12	969
3	418	13	1033
4	600	14	1048
5	667	15	1093
6	690	16	1128
7	751	17	1174
8	780	18	1237
9	826	19	1258
10	844	20	1288

[a]These results are obtained by scanning the laser frequency in a small range around each resonance and recording the laser frequency from the wave meter. Each marked center frequency has an uncertainty of about 3 MHz due to the ambiguity in vertical offset of the MTS signal. We note that the frequency difference between the fourth line and the barium resonance of the $P_{1/2} - D_{3/2}$ transition is known to be 593 (±30) MHz [31,34], which is consistent with our measurement result of 600 (±6) MHz. The experimental uncertainty is about 6 MHz in total, where 3 MHz comes from the vertical offset, and 5 MHz comes from the fitting errors shown in Figs. 5 and 6.

we observe the dark resonances occur at −54, −40, −31, and −18 MHz, which are in agreement with the theoretical expectation of Eq. (5).

From these experimental results, we find that the resonance frequency of the $P_{1/2} - D_{3/2}$ transition is 350 MHz lower than the frequency of the first line of I_2 line in Fig. 2, which is close enough for an AOM to bridge in further experiments. Additionally, we list center frequencies of the 20 lines of I_2 in Table 1 in terms of their offsets from the $P_{1/2} - D_{3/2}$ transition frequency of a single $^{138}Ba^+$ ion.

4. CONCLUSION

We have implemented the MTS of I_2 around 650 nm for the trapped Ba^+ ion experiment. We report 20 lines of I_2 in the vicinity of the $P_{1/2} - D_{3/2}$ transition of the Ba^+ ion, and we have accomplished the stabilization of the 650 nm laser by using one of these lines as the absolute reference. We also have performed the spectroscopy of a single $^{138}Ba^+$ ion and concluded that the resonance of the $P_{1/2} - D_{3/2}$ transition is 350 MHz lower than the lowest absolute reference line among the 20 observed lines of I_2. Our development will enable us to perform precise experiments with Ba^+ ion including sub-Doppler cooling for quantum computation or precision measurement [35].

Funding. National Key Research and Development Program of China (2016YFA0301900, 2016YFA0301901); National Natural Science Foundation of China (NSFC) (11374178, 11574002);.

Acknowledgment. We are grateful to Margaret Pavlovich for her comments on the manuscript.

REFERENCES

1. J. Cirac and P. Zoller, "Quantum computations with cold trapped ions," Phys. Rev. Lett. **74**, 4091–4094 (1995).
2. H. Häffner, C. Roos, and R. Blatt, "Quantum computing with trapped ions," Phys. Rep. **469**, 155–203 (2008).
3. C. Monroe and J. Kim, "Scaling the ion trap quantum processor," Science **339**, 1164–1169 (2013).
4. C. Schneider, D. Porras, and T. Schaetz, "Experimental quantum simulations of many-body physics with trapped ions," Rep. Prog. Phys. **75**, 024401 (2012).
5. R. Blatt and C. F. Roos, "Quantum simulations with trapped ions," Nat. Phys. **8**, 277–284 (2012).
6. G. Kirchmair, F. Zähringer, R. Gerritsma, M. Kleinmann, O. Gühne, A. Cabello, R. Blatt, and C. F. Roos, "State-independent experimental test of quantum contextuality," Nature **460**, 494–497 (2009).
7. C.-W. Chou, D. Hume, T. Rosenband, and D. Wineland, "Optical clocks and relativity," Science **329**, 1630–1633 (2010).
8. X. Zhang, M. Um, J. Zhang, S. An, Y. Wang, D.-l. Deng, C. Shen, L.-M. Duan, and K. Kim, "State-independent experimental test of quantum contextuality with a single trapped ion," Phys. Rev. Lett. **110**, 070401 (2013).
9. R. Drever, J. L. Hall, F. Kowalski, J. Hough, G. Ford, A. Munley, and H. Ward, "Laser phase and frequency stabilization using an optical resonator," Appl. Phys. B **31**, 97–105 (1983).
10. I. Velchev, R. van Dierendonck, W. Hogervorst, and W. Ubachs, "A dense grid of reference iodine lines for optical frequency calibration in the range 571–596 nm," J. Mol. Spectrosc. **187**, 21–27 (1998).
11. S. Xu, R. van Dierendonck, W. Hogervorst, and W. Ubachs, "A dense grid of reference iodine lines for optical frequency calibration in the range 595–655 nm," J. Mol. Spectrosc. **201**, 256–266 (2000).
12. J. L. Hall, L.-S. Ma, M. Taubman, B. Tiemann, F.-L. Hong, O. Pfister, and J. Yes, "Stabilization and frequency measurement of the I_2 stabilized Nd:YAG laser," IEEE Trans. Instrum. Meas. **48**, 583–586 (1999).
13. F. Bertinetto, P. Cordiale, S. Fontana, and G. B. Picotto, "Helium-neon lasers stabilized to iodine at 605 nm," IEEE Trans. Instrum. Meas. **IM-36**, 609–612 (1987).
14. P. Cerez and S. Bennett, "Helium-neon laser stabilized by saturated absorption in iodine at 612 nm," Appl. Opt. **18**, 1079–1083 (1979).
15. J. Lazar, O. Cíp, and P. Jedicka, "Tunable extended-cavity diode laser stabilized on iodine at 633 nm," Appl. Opt. **39**, 3085–3088 (2000).
16. H. Ludvigsen and C. Holmlund, "Frequency stabilization of a GaA1As semiconductor laser to an absorption line of iodine vapor," Rev. Sci. Instrum. **63**, 2135–2137 (1992).
17. S. Olmschenk, K. Younge, D. Moehring, D. Matsukevich, P. Maunz, and C. Monroe, "Manipulation and detection of a trapped Yb^+ hyperfine qubit," Phys. Rev. A **76**, 052314 (2007).
18. D. W. Preston, "Doppler-free saturated absorption: laser spectroscopy," Am. J. Phys. **64**, 1432–1436 (1996).
19. D. McCarron, S. King, and S. Cornish, "Modulation transfer spectroscopy in atomic rubidium," Meas. Sci. Technol. **19**, 105601 (2008).
20. L. Slodicka, G. Hétet, N. Röck, P. Schindler, M. Hennrich, and R. Blatt, "Atom-atom entanglement by single-photon detection," Phys. Rev. Lett. **110**, 083603 (2013).
21. J. Wright, C. Auchter, C.-K. Chou, R. D. Graham, T. Noel, T. Sakrejda, Z. Zhou, and B. B. Blinov, "Scalable quantum computing architecture with mixed species ion chains," Quantum Inf. Process. **15**, 5339–5349 (2016).
22. C. Auchter, C.-K. Chou, T. W. Noel, and B. B. Blinov, "Ion-photon entanglement and bell inequality violation with $^{138}Ba^+$," J. Opt. Soc. Am. B **31**, 1568–1572 (2014).
23. N. Fortson, "Possibility of measuring parity nonconservation with a single trapped atomic ion," Phys. Rev. Lett. **70**, 2383–2386 (1993).
24. J. A. Sherman, W. Trimble, S. Metz, W. Nagourney, and N. Fortson, "Progress on indium and barium single ion optical frequency standards," in *Digest of the LEOS Summer Topical Meetings* (2005), pp. 99–100.
25. G. Shu, M. Dietrich, N. Kurz, and B. Blinov, "Trapped ion imaging with a high numerical aperture spherical mirror," J. Phys. B **42**, 154005 (2009).
26. D. Munshi, "Precision measurement of branching fractions of $^{138}Ba^+$," Phys. Rev. A **91**, 040501 (2015).
27. C. Raab, J. Bolle, H. Oberst, J. Eschner, F. Schmidt-Kaler, and R. Blatt, "Diode laser spectrometer at 493 nm for single trapped Ba^+ ions," Appl. Phys. B **67**, 683–688 (1998).
28. M. Dietrich, "Barium ions for quantum computation," Ph.D. thesis (University of Washington, 2009).
29. R. Lechner, C. Maier, C. Hempel, P. Jurcevic, B. P. Lanyon, T. Monz, M. Brownnutt, R. Blatt, and C. F. Roos, "Electromagnetically-induced-transparency ground-state cooling of long ion strings," Phys. Rev. A **93**, 053401 (2016).
30. S. Ejtemaee and P. Haljan, "3D sisyphus cooling of trapped ions," Phys. Rev. Lett. **119**, 043001 (2017).
31. T. Huber, "Optical trapping of barium ions-towards ultracold interactions in ion-atom ensembles," Ph.D. thesis (Albert-Ludwigs-Universität Freiburg, 2014).
32. H. Oberst, "Resonance fluorescence of single barium ions," Ph.D. thesis (Innsbruck University, 1999).
33. M. O. Scully and M. S. Zubairy, *Quantum Optics* (AAPT, 1999).
34. H. Karlsson and U. Litzén, "Revised ba i and ba ii wavelengths and energy levels derived by Fourier transform spectroscopy," Phys. Scripta **60**, 321–328 (1999).
35. J. Eschner, G. Morigi, F. Schmidt-Kaler, and R. Blatt, "Laser cooling of trapped ions," J. Opt. Soc. Am. B **20**, 1003–1015 (2003).